



Evaluation of the aniline chemical oxidation process using multiple simultaneous electrochemical responses

Fernando H. Cristovan^a, Sherlan G. Lemos^b, Janaína S. Santos^a, Francisco Trivinho-Strixino^a, Ernesto C. Pereira^{a,*}, Luiz H.C. Mattoso^c, Rashmi Kulkarni^d, Sanjeev K. Manohar^d

^a Laboratório Interdisciplinar de Eletroquímica e Cerâmica, Departamento de Química, Universidade Federal de São Carlos, CP 676, 13560-970, São Carlos, SP, Brazil

^b Departamento de Química, Universidade Federal da Paraíba, CP 5093, 58051-970, João Pessoa, PB, Brazil

^c Laboratório Nacional de Nanotecnologia para o Agronegócio, Embrapa Instrumentação Agropecuária, CP 741, CEP 13560-970, São Carlos, SP, Brazil

^d Department of Chemical Engineering, One University Avenue, Room EB 106, University of Massachusetts Lowell, MA 01854, USA

ARTICLE INFO

Article history:

Received 22 October 2009

Received in revised form 8 February 2010

Accepted 13 February 2010

Available online 20 February 2010

Keywords:

PANI

Chemical synthesis

Potentiometry

EQCM

Impedance spectroscopy

ABSTRACT

In this paper we show the simultaneous evaluation of the electrochemical impedance, the open circuit potential and the mass variation of the polyaniline deposited on a metal substrate during chemical oxidation of aniline. We detected that the final properties of the polymer could be practically defined after the inflection point of the potential profile. Considering a series connection of R and C , impedance Z was decomposed into the resistive and capacitive components. The resistivity and permittivity show a slight change after the inflection point in the potential profile. Impedance data and mass changes during synthesis also contributed to a better definition of the induction period. We described the system as whole, which relates to an electronic transport and to an electronic charge storage process. Although very simple, this model helps us to interpret and correlate different techniques to explain the results. In addition, we demonstrated that the *in situ* evaluation of the parameters described above offers new insights on the chemical synthesis mechanism of polyaniline.

© 2010 Elsevier Ltd. All rights reserved.

1. Introduction

The discovery of “synthetic metals” started a new research frontier in the scientific community focussed on the investigation of the synthesis and properties of intrinsically conducting polymeric materials. A significant portion of these studies has been devoted to polyaniline (PANI), which is claimed to be the most versatile conducting polymer due to its high conductivity, redox properties, low cost, easy preparation and environmental stability [1–3]. The stability of polyaniline is of great interest for many different technological applications; various forms of polyaniline have been used as components in organic electronic devices [4], gas separating membranes [5], electromagnetic shielding, antistatic coatings, heaters [6] and components for electrochemical sensors [7].

PANI and its derivatives are generally synthesized by chemical or electrochemical oxidative polymerization of the monomers, although some other approaches, such as plasma polymerization [8,9], electroless polymerization [10], and solid-state polymerization [11], have also been reported. Among them, the chemical oxidation process is particularly important because it is the most feasible method to produce polyaniline powder on a large scale.

Several papers [12–20] focus on this process due to the fundamental interest in the reaction mechanism as well as in the PANI thin layer deposition phenomenon on different surfaces [21,22]. The aniline polymerization reaction was proposed to proceed via the formation of dimer molecules during the initiation process, which is followed by their oligomerization in the early stages of polymer growth [16,18–20]. Once oligomers in the pernigraniline oxidation state [17] are produced, the chain is proposed to grow via an autocatalytic mechanism in which the remaining aniline is oxidized by the pernigraniline and added to the growing polymer chain [20].

The main method used to monitor the evolution of polyaniline chemical synthesis is to follow the open circuit potential (V_{oc}) of a working electrode placed in the polymerization solution [17]. However, this technique does not supply much information on the reactions occurring during polymer formation. Epstein and co-workers [17] proposed that the maximum V_{oc} profile is related to the existence of the pernigraniline oxidation state, and the reaction ends when the V_{oc} has almost no variation, where polyaniline in the emeraldine oxidation state is obtained. Other techniques, such as electrochemical quartz crystal microbalance (EQCM) and electronic absorption spectrometry, were used to follow this reaction [12,23–25]. In general, these studies [12,23–25] aimed at the evaluation of the experimental conditions to obtain PANI with higher molecular weights and suitable electrical properties, leaving a gap in the investigation of the synthesis mechanism.

* Corresponding author. Tel.: +55 16 3361 5215; fax: +55 16 3351 8214.
E-mail address: decp@power.ufscar.br (E.C. Pereira).

However, an important contribution that can be obtained from the EQCM/UV–vis studies is the definition of the induction period on the oxidative chemical polymerization of aniline [12,23–25].

As will be shown in this paper, electrochemical impedance spectroscopy (EIS) is a technique that can also be used to follow the aniline chemical oxidation process. The established theoretical background and experimental conditions make EIS a convenient and readily available tool for obtaining important chemical information of a system, even in a chemical process, as the small ac voltage perturbation does not significantly modify the reaction rate [26–31]. Few articles have been found describing the application of EIS for the characterization of the electrochemical behaviour of polyaniline films prepared by chemical synthesis [32–36]. Moreover, none of these articles focus on monitoring the aniline chemical oxidation process and the transformations that occur. To the best of our knowledge, no work has been done systematically investigating this matter. Therefore, in the present paper we evaluate simultaneously the electrochemical impedance, the open circuit potential and the mass variation of the PANI deposited on a metal substrate during the chemical oxidation of aniline.

2. Experimental

All reagents used in this work were of analytical grade and used as received, unless otherwise described. All solutions were prepared with deionised water ($R = 18 \text{ M}\Omega \text{ cm}^{-1}$). Aniline (Mallinckrodt) was distilled under reduced pressure resulting in a colourless liquid.

Polyaniline powder was prepared by chemical oxidation based on a procedure adapted from the standard one [37]. Two solutions (A and B) were prepared in advance. Solution A was 270 mL of 1 mol L^{-1} aqueous HCl solution containing 3.2×10^{-3} moles of aniline. Solution B was 20 mL of an aqueous solution containing 8.0×10^{-4} moles of ammonium persulfate (APS) (Mallinckrodt) as oxidant, which corresponds to a 0.25 molar ratio of APS to aniline. A 400 mL jacketed flat-bottom reactor was used to prepare the polymer. This flask was kept under stirring and thermostated at 0°C by using a circulating chiller unit Polystat (Cole Parmer, United States) equipped with an ethylene glycol/water mixture as coolant. Both solutions A and B were thermally equilibrated to 0°C . Next, solution A was transferred into this reactor, to which solution B at 0°C was then rapidly poured onto and mixed with solution A. The mixture was kept under continuous stirring at 0°C for 2 h. The progress of the chemical oxidation of aniline by APS was monitored by open circuit potential, EQCM measurements, and electrochemical impedance, as described below. It is well known [38] that freshly collected PANI by this procedure yields PANI in emeraldine salt (ES) form ($\sim 50\%$ of reduced amine and 50% of oxidized imine monomers, and a protonation degree of $\sim 42\%$).

The open circuit potential of the synthesis was constantly measured using the potential profiling technique described elsewhere [17].

The EQCM measurements were carried out using a Seiko EG&G Quartz Crystal Analyzer (model QCA 917) coupled to a potentiostat/galvanostat model EG&G PAR 263A. For the EQCM measurements, a 9 MHz 'AT-cut' quartz crystal coated with platinum film was used as working electrode (WE) and resonator. This electrode was placed in a vertical position and the area of the electrode used for PANI deposition was 0.2 cm^2 . The counter electrode (CE) was a Pt sheet with an area of 0.5 cm^2 , and a saturated calomel electrode (SCE) was used as reference electrode. All three electrodes were placed parallel to each other. The quartz crystal was mounted in a Teflon® holder, immersed in the solution, and connected to an oscillator circuit isolated from the solution. Only one side of the crystal was exposed to the electrolyte solution. Prior to use, the

electrodes were cleaned by ultrasonic treatment in acetone and by sulfonitric solution (1:1 mixture of conc. HNO_3 /conc. H_2SO_4 , v/v), then rinsed thoroughly with pure water, and dried in a nitrogen gas flow.

The mass per unit area of the PANI film, Δm (g cm^{-2}), grown onto the platinum-coated quartz crystal electrode of EQCM, was determined from the change in its resonance frequency. The frequency decreases linearly with the increasing mass deposited onto the electrode. The relation between the frequency change Δf (Hz) and Δm is well established by Sauerbrey [39] as given below:

$$\Delta f = -\frac{2f_0^2}{A\sqrt{\rho_Q\mu_Q}}\Delta m = -K\Delta m \quad (1)$$

where f_0 (Hz) is the natural frequency of the quartz crystal, ρ_Q the quartz density (2.649 g cm^{-3}), μ_Q the shear modulus ($2.947 \times 10^{11} \text{ g cm}^{-1} \text{ s}^{-2}$), and K is the experimental mass coefficient or sensitivity coefficient. The sensitivity of the EQCM used was $858.8 \text{ Hz } \mu\text{g}^{-1}$.

For the impedance experiments, an interdigitated working electrode was used in such way that the polymer electronic properties were measured between the two contacts in the back side of the formed polymer. This was fabricated from two gold sputtered parts in a comb-shape configuration on glass fibre substrate. Before use, the interdigitated electrode was cleaned by ultrasonic treatment in acetone and by sulfonitric solution, then rinsed thoroughly with purified water, and dried in a nitrogen gas flow. The impedance measurements were carried out using a frequency response analyzer, Shlumberger Solartron Analyzer (model 1260). Impedance data were obtained using an ac potential of 50 mV rms and a frequency of 1 kHz at the same time as the open circuit potential measurements (above), but using different equipments and experimental setup. In the analyzed frequency region (1 kHz) the dominant process is associated with the electronic process. Additionally, there is no dependence of the form of the impedance curve on the frequency and the amplitude when $2 \text{ Hz} < f < 2000 \text{ Hz}$ [40]. The capacitances obtained are related to the bulk and interface properties of the system.

An electroacoustic impedance study carried out within the 2-h synthesis as described elsewhere [41]. The crystal admittance spectra were collected in the frequency range 8.98–9.0275 MHz, in order to ensure that the frequency change in the EQCM experiments was not affected by changes in viscoelastic properties of PANI during PANI film growing process, and to validate the use of Eq. (1) on relating frequency change and the mass variation. The conformity to acoustically thin film ("rigidly coupled") conditions was determined by acquisition of crystal admittance spectra using a Shlumberger Solartron Analyzer (model 1260) [41], as shown in Fig. 1. The admittance spectra acquired during polymer synthesis show a small change in the admittance peak and width, as it is shown in Fig. 1. This behaviour is characteristic of rigid films, i.e. the morphology change of the coating polymer does not significantly affect the admittance of the oscillating quartz crystal. As no viscoelastic changes were observed, i.e. film rigidity changes and swelling effects were negligible for the thin film studied here, Sauerbrey's equation was used. In fact, the results presented in Fig. 1 are in agreement with those in the literature [41,42].

3. Results and discussion

Fig. 2 depicts the open circuit potential and mass polymer growth profiles. Upon the addition of solution B (APS solution), the initial potential of the anilinium hydrochloride solution (solution A) increases to 0.78 V, in agreement with data reported in the literature to the potential for aniline oxidation in a $1 \text{ mol L}^{-1} \text{ H}^+$ solution [20,43]. Then the potential falls to a minimum value at 0.69 V after

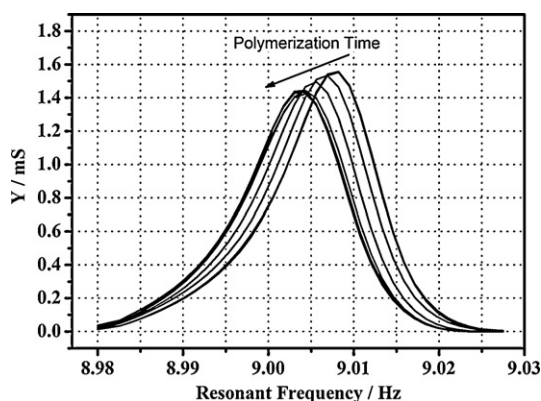


Fig. 1. Crystal admittance spectra recorded during PANI film growth at the top of the electrode, occurring during its chemical polymerization.

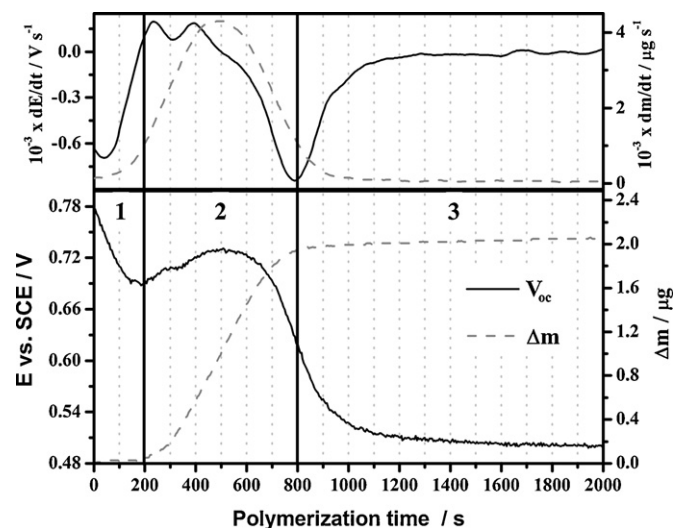


Fig. 2. Open circuit potential profile and mass change during PANI polymerization. Three distinct regions can be perceived: (1) induction period, (2) change of polymerization mechanism, and (3) synthesis termination. At the top is shown the first derivative of open circuit potential and mass curves.

the first 200 s (Fig. 2, region 1). In this stage the reacting mixture takes on a pink tint. This fact is evidence of the formation in the solution of oligomeric cation radicals of aniline [44], i.e. deprotonated anilinium cations oxidized to radical cations and possibly also to nitrenium cations in agreement with the reactions illustrated in Scheme 1 [13].

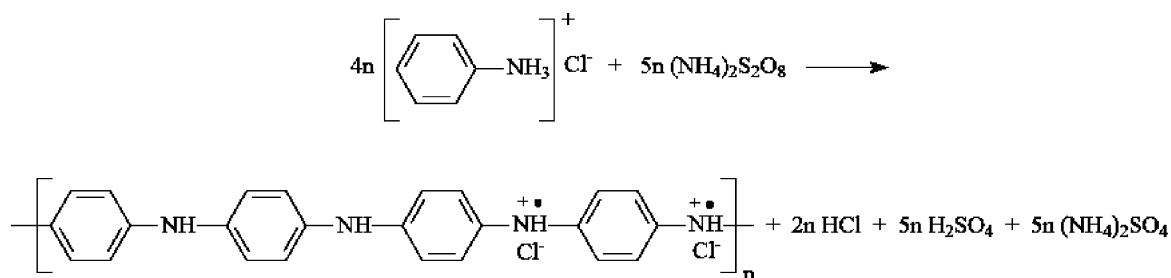
Oligomer formation occurs as the potential decreases to 0.69 V, which is the formal potential corresponding to the oxidation of intermediate species under the synthesis conditions used here [13]. However, dimeric species like *p*-aminodiphenylamine and benzidine, earlier identified at this synthesis stage [20], present oxidation

potentials considerably lower (0.4–0.5 V). Furthermore, other intermediate species such as *N*-phenyl-1,4-benzoquinonediimine (PBQ) [20] – the oxidized form of *p*-aminodiphenylamine – could be present at this stage in addition to the first pernigraniline molecules.

On the other hand, as can be seen in the mass profile at the same stage, region 1, no significant mass variation is observed in this period, indicating that the reaction occurs in the solution phase. This initial stage in the synthesis process is denominated induction period [23–25]. In addition, this stage has been reported in the literature as the period preceding aniline polymerization where the temperature is invariable [45]. At this stage, the adsorbed radical cations formed on the electrode surface start to react with others in their vicinity [46]. Thus, the induction period is strictly related to the formation of low molecular weight intermediates capable of initiating polymer growth, as described above. It has also been reported in the literature that the induction period is influenced by various parameters, such as reactant concentrations, temperature and stirring conditions of the solution [23–25,47].

In the subsequent interval denominated region 2, presented in Fig. 2, the mass curve shows an increase, which is obviously related to polymer growth. It starts at 200 s and the mass deposited over the electrode increases up to 800 s. Taking into account the mass change in this region, a growth rate of 4.2 ng s^{-1} could be estimated. The initiation of the polymer film growth corresponds to the beginning of the increase of potential from 0.69 V reaching a maximum value at 0.73 V after 500 s. Some authors have observed that the pH decreases during this stage [13] and the temperature rises gradually [13,17,18,48], indicating that the oxidative polymerization of aniline is an exothermic process. The pH decrease was attributed by Beadle et al. [13] to polymerization occurring via an autocatalytic mechanism acting simultaneously with chain polymerization, which is the dominant mechanism due to the existence of a sufficiently high concentration of APS. In this chain mechanism the oxidized aniline oligomers catalyze the oxidation of aniline molecules to radical cations or link aniline molecules [13]; similarly, the reduced oligomers are oxidized again by the remaining APS [49]. Thus, polymerization proceeds and ammonium persulfate is available to oxidize the growing chains.

After 400 s of polymerization, a maximum was also observed where the V_{oc} reaches 0.73 V. This potential is characteristic of the formation of polyaniline in its fully oxidized pernigraniline state [17], at which point the solution becomes purple. In previous work [17] it was found that the polymer extracted at this point is analytically pure pernigraniline. It is worth noting that the maximum potential value in this region matches with the inflection point of the mass curve as depicted in Fig. 2 in the first derivative parameters for mass and potential changes. This suggests a change in the dominant mechanism of film growth from chain polymerization to autocatalytic polymerization. At this point, the APS was essentially completely consumed, as determined quantitatively by titrimetric analysis by Epstein and co-workers [17], in agreement with the above proposition. In addition, it is also described in the literature



Scheme 1. Oligomeric cation radicals of aniline formation.

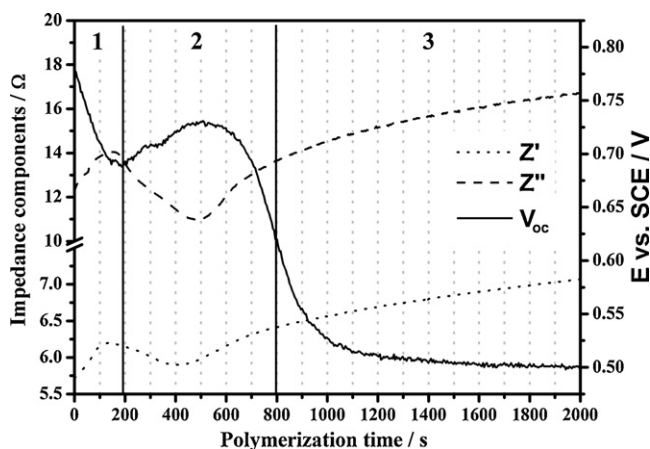


Fig. 3. Variation of the impedance components (Z' : dotted line, Z'' : dashed line) measured during PANI synthesis and open circuit potential profile (solid line).

that the sharp decrease in pH [13] (much larger than in the previous stages) and the abrupt rise of the temperature [13,48,51] also characterize the predominance of the autocatalytic mechanism [52]. After 500 s of polymerization a decrease in the potential value was observed, which is related to the reduction of pernigraniline species by the excess of anilinium chlorhydrate.

It can be also observed (Fig. 2), that the border between regions 2 and 3 matches with the inflection point of the V_{oc} curve and also to the end of the mass increase. It has been reported in the literature that all the polymer has already been obtained at this point, as observed by monitoring yield as a function of polymerization time [50]. It has also been observed [13,52] that it matches with the point of maximum temperature in the growth/reduction stage. Therefore, from our results and those described in the literature [13,50,52], we can propose that the most polymer chain growth occurs during the transition from regions 2 to 3.

As the polymerization proceeds (region 3) the V_{oc} decreases slowly and, after 1800 s, it apparently becomes constant at 0.49 V (Fig. 2). This potential is characteristic of emeraldine oxidation state formation [38]. Similarly, after 800 s, the PANI film mass shows only 5% growth compared to the former stage (region 2). This is consistent with the literature, which has shown that the molecular weight and the yield rise slightly with time during this polymerization stage [53]. Hence, in agreement with the authors, a minimum reaction time of about 15 h is necessary at -26°C to complete the polymerization [53], whereas about 4 h at 0°C [54], and several days at -50°C [55]. Beadle et al. [13] observed an increase in solution pH at this stage and suggested an intake of protons and chloride ions in the PANI backbone transforming emeraldine species to its salt form. In summary, considering our results on potential mass data and the literature data discussed above, we propose that most polymer chain growth occurs up to 800 s, after which stabilization of the polymer oxidation state predominates.

We also collected *in situ* impedance data in order to evaluate the electronic property variation of the polymer during the synthesis. Although the impedance measurements set an ac voltage on the system, this perturbation is low enough not to disturb the growth process, as the V_{oc} profiles and values were insensitive to variations in the applied ac voltage amplitude. The real and imaginary components (Z' and Z'' , respectively) measured are presented in Fig. 3. Generally, the up to date discussion of impedance data in the literature [56–58] has been based on the assumption that there is no geometry variation in the sample. This is certainly not the case during the PANI chemical synthesis as a mass increase occurs on the electrode. Therefore, any analysis of the raw impedance data could lead to a false interpretation of its physical meaning. Considering

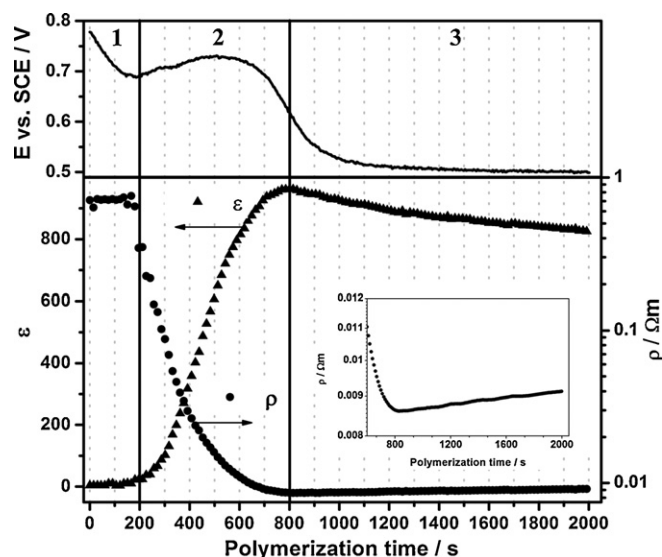


Fig. 4. Permittivity and resistivity as a function of polymerization time. Also shown is the V_{oc} profile and, in an expanded view, the final stage of polymerization, where a small increase of resistivity is observed.

this, we used the mass curve to normalize the impedance data, assuming that the polymer density is constant during the growth. In addition, the ac impedance Z was decomposed into the resistive R and the capacitive C components, proposing that the material can be described as a series connection of R and C [59]. Using data obtained from monitoring the growth of the PANI film by the EQCM technique, the geometric component presented in the impedance results can be evaluated. It is known that the impedance of a sample is the product of the complex resistivity and the length and area ratio, L/A [27]. Considering Z' equal to R , the resistivity (ρ) of the PANI film during synthesis was calculated from:

$$\rho = R \frac{A}{L} \quad (2)$$

In the same way, considering Z'' equal to $1/(2\pi fC)$ and the interdigitated electrode/PANI film system as a parallel-plate capacitor constructed of two parallel plates of area A separated by a distance L , one can estimate a conditional PANI film permittivity (ε) variation during synthesis as follows:

$$\varepsilon = \frac{L}{2\pi f A \varepsilon_0 Z''} \quad (3)$$

where ε_0 is the dielectric permittivity of free space, 8.854×10^{-12} F/m. In the above equations A is the electrode surface area, and the film thickness was adopted as the sample length, L . The film thickness L was determined considering the density of the PANI hydrochloride to be 1.33 g/cm³, as previously determined in the literature [45].

Fig. 4 shows that the resistivity and the permittivity change during the course of the polymerization. Both curves show an initial plateau related to the induction period where no significant polymer formation is observed. After that, a large variation of both parameters is observed, which is related to the film growth (region 2), where resistivity values decrease while the permittivity increases. Permittivity starts to increase as the film is produced and reaches its maximum value at the inflection point, which occurs at the end of region 2. After 800 s (region 3) the permittivity showed a small decrease. It was also observed in region 3 that the resistivity presented a small increase (0.03%), which can be disregarded (Fig. 4, insert).

The permittivity changed during the whole process. Literature data show that the highest value of permittivity could be associ-

ated with the long-range orbital delocalization [60]. After 800 s, the negative slope in permittivity vs. time curve (region 3) could be related to a polymer volume change, which occurs after the polymer oxidation state changes [61,62]. This volume change can be assumed as a “final structure relaxation” due to the intake of electrolyte molecules (water and counter-ions) in the polymer film and the relaxation of the polymer chains caused by the molecule diffusion. This fact could also explain the small mass increase after 800 s observed in Fig. 2.

The resistivity data in Fig. 4 seem to have no significance during the induction period. After 200 s, from the beginning of region 2, their values decrease continuously until $9 \times 10^{-3} \Omega \text{ m}$ and remain constant in the subsequent interval (region 3). This resistivity decrease in region 2 could be related to the conversion of pernigraniline (insulating form) to emeraldine salt (conducting form). This observation is consistent with the literature [63]. Wrighton and co-workers [63] investigated PANI conductivity as a function of oxidation state and observed that maximum conductivity occurs at the potential characteristic of the emeraldine state (50% oxidized form), which was approximately 0.49 V. Furthermore, the polymer conductivity decreases when the emeraldine form is reduced or oxidized and the polymer becomes an insulator in the leucoemeraldine (0.1 V) and pernigraniline forms (0.75 V) [50].

In summary, PANI film properties are practically determined when the potential reaches 0.62 V (in 800 s of polymerization), which is the point related to the end of film growth as discussed previously. The variations of the PANI film parameters after this point could be an indication of the transformations that the polymer backbone is passing through.

It is clear from the preceding discussion that a complete and self-consistent picture has emerged from the *in situ* study of PANI polymerization. From this study we were able to demonstrate the induction period parameter and how it is linked to the electronic and physical properties of PANI during its polymerization. The major advantage of *in situ* techniques rather than conventional *ex situ* techniques in PANI synthesis is the possibility to evaluate the physical chemical properties in real time, giving further information about the synthesized polymer and the polymerization mechanism.

4. Conclusions

In this paper, we have reported the results of an investigation about the usage of different *in situ* techniques to monitor PANI chemical synthesis, and we have demonstrated important advantages of these techniques over conventional approaches. The overall polymerization stages were reviewed in the scope of the *in situ* techniques used here and compared with the literature. From V_{oc} and mass changes during synthesis, it was possible to detect a change in the mechanism of polymerization from chain growth to an autocatalytic mechanism. Following the ac impedance and mass variation during PANI synthesis, we were also able to detect that the polymer properties are basically defined in the first stage of polymerization. In addition, the concept of the induction period was clearly defined from global analysis of the results.

Acknowledgements

The authors wish to thank the Brazilian Funding Institutions CNPq, CAPES, FINEP and FAPESP (Proc.: 03/09933-8, Proc.: 05/00453-9) for their financial support. We also acknowledge the support of the University of Texas at Dallas, where part of this study was performed.

References

- [1] E.M. Genies, A. Boyle, M. Lapkowski, C. Tsintavis, *Synth. Met.* 36 (1990) 139.
- [2] A.A. Syed, M.K. Dinesan, *Talanta* 38 (1991) 815.
- [3] D. Zhang, Y. Wang, *Mater. Sci. Eng. B* 134 (2006) 9.
- [4] G. Gustafsson, Y. Cao, G.M. Treacy, F. Klavetter, N. Colaneri, A.J. Heeger, *Nature* 357 (1992) 477.
- [5] A.J. Conklin, T.M. Su, S.-C. Huang, R. Kaner, in: R.L. Skotheim, R. Elsenbaumer (Eds.), *Handbook of Conducting Polymer*, Marcel Dekker, New York, 1998.
- [6] H.H. Kuhn, A.D. Child, in: R.L. Skotheim, R. Elsenbaumer (Eds.), *Handbook of Conduction Polymers*, Marcel Dekker, New York, 1998.
- [7] T. Lindfors, A. Ivaska, *J. Electroanal. Chem.* 531 (2002) 43.
- [8] L.G. Paterno, S. Manolache, F. Denes, *Synth. Met.* 130 (2002) 85.
- [9] G.J. Cruz, J. Morales, M.M. Castilloortega, R. Olayo, *Synth. Met.* 88 (1997) 213.
- [10] C.P. Liao, M.Y. Gu, *Thin Solid Films* 408 (2002) 37.
- [11] J.X. Huang, J.A. Moore, J.H. Acquaye, R.B. Kaner, *Macromolecules* 38 (2005) 317.
- [12] M.M. Ayad, M.A. Shenashin, *Eur. Polym. J.* 39 (2003) 1319.
- [13] P.M. Beadle, Y.F. Nicolau, E. Banka, P. Rannou, D. Djurado, *Synth. Met.* 95 (1998) 29.
- [14] L.H.C. Mattoso, S.K. Manohar, A.G. MacDiarmid, A.J. Epstein, *J. Polym. Sci. Polym. Chem.* 33 (1995) 1227.
- [15] J. Stejskal, P. Kratochvíl, M. Spirkova, *Polymer* 36 (1995) 4135.
- [16] B.J. Johnson, S.M. Park, *J. Electrochem. Soc.* 143 (1996) 1277.
- [17] S.K. Manohar, A.G. MacDiarmid, A.J. Epstein, *Synth. Met.* 41 (1991) 711.
- [18] I. Sapurina, A. Riede, J. Stejskal, *Synth. Met.* 123 (2001) 503.
- [19] K. Sasaki, M. Kaya, J. Yano, A. Kitani, A. Kunai, *J. Electroanal. Chem.* 215 (1986) 401.
- [20] N. Gospodinova, L. Terlemezyan, *Prog. Polym. Sci.* 23 (1998) 1443.
- [21] A.G. MacDiarmid, A.J. Epstein, *Faraday Discuss.* 88 (1989) 317.
- [22] R. Mazeikiene, A. Malinauskas, *J. Chem. Res. S* (1999) 622.
- [23] M.M. Ayad, M.A. Shenashin, *Eur. Polym. J.* 40 (2004) 197.
- [24] M.M. Ayad, A.H. Gemaey, N. Salahuddin, M.A. Shenashin, *J. Colloid Interface Sci.* 263 (2003) 196.
- [25] M.M. Ayad, N. Salahuddin, M.A. Shenashin, *Synth. Met.* 142 (2004) 101.
- [26] H.J. Yang, A.J. Bard, *J. Electroanal. Chem.* 339 (1992) 423.
- [27] E. Barsoukov, J.R. MacDonald, *Impedance Spectroscopy: Theory, Experiment, and Applications*, 2nd ed., Wiley, New Jersey, 2005, p. 606.
- [28] P. Fiordiponti, G. Pistoia, *Electrochim. Acta* 34 (1989) 215.
- [29] C. Deslouis, M.M. Musiani, B. Tribollet, *J. Phys. Chem.* 98 (1994) 2936.
- [30] G.S. Popkurov, E. Barsoukov, R.N. Schindler, *J. Electroanal. Chem.* 425 (1997) 209.
- [31] M.A. Vorotyntsev, J.P. Badiali, G. Inzelt, *J. Electroanal. Chem.* 472 (1999) 7.
- [32] K. Rossberg, L. Dunsch, *Electrochim. Acta* 44 (1999) 2061.
- [33] N.M. Kocherginsky, Z. Wang, *Synth. Met.* 156 (2006) 1065.
- [34] R. Singh, V. Arora, R.P. Tandon, S. Chandra, A. Mansingh, *J. Mater. Sci.* 33 (1998) 2067.
- [35] M. Irimia-Vladu, J.W. Fergus, *Synth. Met.* 156 (2006) 1396.
- [36] A. Benyaich, C. Deslouis, T. Elmoustaïf, M.M. Musiani, B. Tribollet, *Electrochim. Acta* 41 (1996) 1781.
- [37] A.G. MacDiarmid, J.C. Chiang, A.F. Richter, N.L.D. Somarisi, In: L. Alcacer (Ed.), *Conducting Polymers*, Reidel, Dordrecht, 1987, p. 105.
- [38] L.H.C. Mattoso, A.G. MacDiarmid, A.J. Epstein, *Synth. Met.* 68 (1994) 1.
- [39] G. Sauerbrey, *Zeitschrift Für Physik* 155 (1959) 206.
- [40] K. Aoki, K. Hayashi, *J. Electroanal. Chem.* 384 (1995) 31.
- [41] A.R. Hillman, M.A. Mohamoud, *Electrochim. Acta* 51 (2006) 6018.
- [42] H. Yang, J. Kwak, *J. Phys. Chem. B* 101 (1997) 774.
- [43] B.J. Johnson, S.M. Park, *J. Electrochem. Soc.* 143 (1996) 1269.
- [44] K.G. Neoh, E.T. Kang, K.L. Tan, *Polymer* 34 (1993) 3921.
- [45] J. Stejskal, I. Sapurina, J. Prokes, J. Zemek, *Synth. Met.* 105 (1999) 195.
- [46] I. Sapurina, A.Y. Osadchev, B.Z. Volchek, M. Trchova, A. Riede, J. Stejskal, *Synth. Met.* 129 (2002) 29.
- [47] G.P. Karpacheva, A.V. Orlov, S.G. Kiseleva, S.Z. Ozkan, O.Y. Yurchenko, G.N. Bondarenko, *Russ. J. Electrochem.* 40 (2004) 305.
- [48] Y.P. Fu, R.L. Elsenbaumer, *Chem. Mater.* 6 (1994) 671.
- [49] N. Gospodinova, L. Terlemezyan, P. Mokreva, K. Kossev, *Polymer* 34 (1993) 2434.
- [50] L.H.C. Mattoso, *Quim. Nova* 19 (1996) 388.
- [51] Y. Maeda, A. Katsuta, K. Nagasaki, M. Kamiyama, *J. Electrochem. Soc.* 142 (1995) 2261.
- [52] Y. Geng, J. Li, Z. Sun, X. Jing, F. Wang, *Synth. Met.* 96 (1998) 1.
- [53] P.N. Adams, P.J. Laughlin, A.P. Monkman, *Synth. Met.* 76 (1996) 157.
- [54] Y. Cao, A. Andreatta, A.J. Heeger, P. Smith, *Polymer* 30 (1989) 2305.
- [55] J. Stejskal, A. Riede, D. Hlavat, J. Proke, M. Helmstedt, P. Holler, *Synth. Met.* 96 (1998) 55.
- [56] E.S. Matvewa, R. Diaz Callha, V.P. Parkhutik, *Electrochim. Acta* 41 (1996) 1351.
- [57] F. Fusalba, D. Belanger, *Electrochim. Acta* 45 (2000) 3877.
- [58] R. Diaz Calleja, E.S. Matvewa, V.P. Parkhutik, *J. Non-Cryst. Solids* 180 (1995) 260.
- [59] A. Riul Júnior, A.M. Gallardo Soto, S.V. Mello, S. Bone, D.M. Taylor, L.H.C. Mattoso, *Synth. Met.* 132 (2003) 109.
- [60] H.A. Pohl, *J. Electron. Mater.* 15 (1986) 201.
- [61] T.F. Otero, H.J. Grande, J. Rodriguez, *J. Phys. Chem. B* 101 (1997) 3688.
- [62] T.F. Otero, in: H.S. Nalwa (Ed.), *Artificial Muscles, Electrodisolution and Redox Processes in Conducting Polymers*, vol. 4, John Wiley & Sons Ltd., New York, 1997, p. 10.
- [63] D. Ofer, R.M. Crooks, M.S. Wrighton, *J. Am. Chem. Soc.* 112 (1990) 7869.